

Fault-Induced Signal Distortion in FMCW Automotive Radar: Simulation-Based Analysis

Sheriff Murtala¹, Ingyu Lee², Soojung Hur³, and Gyusang Choi⁴

^{1,2,3,4} *Yeungnam University, Gyeongsan, Gyeongbuk 38541, Republic of Korea*

sheriffm@yu.ac.kr

inleeatyu@yu.ac.kr

sjeo@ynu.ac.kr

castchoi@ynu.ac.kr

ABSTRACT

Faults in frequency-modulated continuous wave (FMCW) radar systems can distort the radar signal and compromise system performance, yet their signal-level impacts remain underexplored. This paper presents a simulation-based analysis of signal distortions caused by five representative fault behaviors including noise, gain, negate value, offset, and delay, across three critical FMCW radar subsystems: waveform generator, transmitter, and receiver. We examine the effects of each fault on complex baseband signals and range estimation accuracy, providing both qualitative and quantitative evaluations. The results reveal distinct distortion patterns and demonstrate that range errors and false negatives can occur, prompting the need for diagnostic and fault-aware processing strategies. Notably, noise, delay, and offset faults have the most significant impact on signal integrity and range estimation, while gain and negate value faults showed no measurable degradation in performance.

1. INTRODUCTION

Recent advancements and widespread integration of radar technology across multiple sectors have significantly increased the complexity of associated electronic systems (Moghaddam, Aghdam, Filippi, & Eriksson, 2020). In automotive applications, radar subsystems are typically deployed without ongoing maintenance, making fault detection and mitigation a critical challenge for long-term reliability (Matos, Bernardino, Durães, & Cunha, 2024). The lack of scalable fault detection strategies is especially problematic for autonomous systems that require high reliability.

Frequency Modulated Continuous Wave (FMCW) radar architectures consist of multiple modules (Jankiraman, 2018),

including waveform generators, transmitters, receivers, and digital signal processors, that are inherently susceptible to hardware faults (Wileman & Perinpanayagam, 2013). The nature of these faults varies widely depending on the affected component, leading to diverse failure modes. While hardware-level failures are well documented in existing literature, their direct impact on signal integrity, particularly in terms of distortion, has received comparatively limited attention (Subburaj et al., 2018; Ginsburg et al., 2018). Fault-induced signal anomalies in automotive radar subsystems can degrade range estimation and target detection, compromising both system performance and driving safety. This underscores the need for simulation-based analysis to model and evaluate distortion effects in FMCW radar systems.

Efforts to estimate the remaining useful life (RUL) of radar Transmit/Receive (T/R) modules involved the use of least squares-based parameter identification frameworks to model degradation behavior (Murtala, Lee, & Park, 2023). In parallel, Zhai et al. proposed several data-driven prognostic models for radar transmitters. These include a multivariate Long Short-Term Memory (LSTM) network combined with a multivariate Gaussian distribution for fault prediction (Zhai & Fang, 2020), an unsupervised isolation forest approach for degradation detection (Zhai, Shao, Li, & Fang, 2021), and a hybrid model combining dynamic updated AutoRegressive Integrated Moving Average (ARIMA) with multivariate isolation forest techniques (Zhai, Liu, Cheng, & Fang, 2022). Complementary research also introduced fault prediction models using Vector Autoregression (VAR), enhanced by advanced signal processing methods such as Piecewise Cubic Hermite Interpolation and Wavelet Multivariate Denoising (Murtala, Soojung, & Park, 2023). These methodologies offer robust tools for modeling fault behavior and enhancing the reliability of radar systems, paving the way for predictive maintenance strategies that minimize downtime, reduce operational costs, and ensure sustained performance in mission-critical applications. Similar approaches have been

Sheriff Murtala et al. This is an open-access article distributed under the terms of the Creative Commons Attribution 3.0 United States License, which permits unrestricted use, distribution, and reproduction in any medium, provided the original author and source are credited.

explored in broader industrial contexts, such as automated machine learning frameworks for RUL prediction in cyber-physical systems (Zöller, Mauthe, Zeiler, Lindauer, & Huber, 2025) and deep learning-based degradation modeling for aerospace systems (Darrah, Lövberg, Frank, & Quinones-Gruiero, 2022).

Beyond internal subsystem faults, radar performance is also compromised by physical misalignments, which alter the beam orientation of signals and reduce accuracy in object detection. A comprehensive survey on radar misalignment detection highlights the impact of vertical and horizontal deviations on system reliability, particularly in safety-critical scenarios (Sharif, Murtala, & Choi, 2025). These misalignments, while mechanical in nature, share common consequence with electronic fault, both induce signal anomalies that degrade radar functionality. The implications of radar faults extend beyond technical performance to broader safety outcomes (Burza, 2024). A machine learning-based study on accident severity prediction demonstrates how sensor faults, including radar sensors, influence the likelihood and severity of vehicular collisions (Matos et al., 2024; Shafique, Rustam, Murtala, Jurcut, & Choi, 2024). Additionally, recent work on ghost object detection has revealed how signal anomalies, whether caused by hardware faults, environmental interference, or adversarial spoofing, can lead to false positives in object recognition, posing serious risks to autonomous navigation and decision-making (Kraus, Scheiner, Ritter, & Dietmayer, 2021; Murtala, Hur, & Park, 2025). These findings reinforce the need for robust fault modeling and signal integrity analysis.

This study presents a simulation-based analysis of five representative fault behaviors induced across three critical subsystems of automotive radar, the waveform generator, transmitter, and receiver. It investigates how these faults affect the integrity of complex radar signals and compromise the accuracy of range estimation. The analysis includes both quantitative evaluations, assessing impact through performance metrics, and qualitative assessments that characterize the nature and structure of the observed distortions. By integrating these complementary approaches, the study offers a comprehensive view of how subsystem faults manifest at the signal level and influence downstream radar processing performance. The analysis advances fault modeling in automotive radar and supports the development of predictive maintenance strategies.

This paper is organized as follows: Section 2 introduces the FMCW radar architecture and operational principles, and reviews common fault types along with related literature. Section 3 details the simulation-based methodology. Section 4 presents and analyzes the results. Finally, Section 5 concludes the paper and outlines potential directions for future research.

2. BACKGROUND

2.1. Common Fault Types in Radar System

The reliable operation of radar system depends on the coordinated performance of its key subsystems, including the waveform generator, transmitter, receiver, and digital signal processor. Each of these components is susceptible to specific degradation mechanisms that can impair overall system performance. If left undetected, such degradations may lead to severe consequences, including reduced resolution, shortened detection range, and increased false alarm rates. This section reviews common fault types observed in radar systems, outlining their underlying physical causes and the operational precursors that often signal their presence.

Wileman and Perinpanayagam conducted a comprehensive analysis of fault mechanisms in radar and radio frequency (RF) systems, applying Failure Modes, Effects, and Criticality Analysis (FMECA) to identify high-risk components (Wileman & Perinpanayagam, 2013). Their study linked semiconductor wear-out and other degradation processes to system-level health indicators, and established a framework for Prognostics and Health Management (PHM) planning grounded in physics-of-failure principles.

Kulevome et al. developed a PHM framework tailored to radar systems, emphasizing operational fidelity and system-level diagnostics (Kulevome et al., 2021). Their methodology involved identifying critical subsystems, deploying sensors, and modeling degradation to estimate Remaining Useful Life (RUL). Although the paper did not explicitly describe the use of FMEA, its structure aligned with fault isolation and performance monitoring strategies. Sensor data were processed to support fault detection and enable adaptive maintenance planning.

Hou et al. proposed a data-driven technique for selecting degradation-sensitive parameters in phased array radar transmitter/receiver modules (Hou et al., 2018). Their method targeted fault precursors specific to the transmitter and receiver subsystems using association rule mining, which filtered out variables with weak statistical relevance to fault modes. By calculating support and confidence metrics from Built-In Test Equipment (BITE) data, the authors identified key indicators such as output power, transmitter channel gain, noise coefficient, and stray signal suppression. These parameters reflected degradation under transmitter, receiver, or combined fault conditions. The approach reduced RUL estimation error and improved fault detection accuracy at the module level, thereby strengthening predictive maintenance capabilities.

Bak and Kim extended prior methodologies by introducing a data-driven approach for identifying potential antenna defects during the radar manufacturing process (Bak & Kim, 2023). Their objective was to mitigate degradation in transmitter and receiver subsystems by addressing faults at the production

stage. The authors formulated the task as a multi-output regression problem and addressed multicollinearity by employing ensemble learning techniques, including Random Forest, LightGBM, Gradient Boosting, Ridge, and Lasso models. The modeling pipeline was implemented using AutoML via PyCaret, which facilitated automated feature selection, model training, and hyperparameter optimization. The final ensemble model achieved mean absolute error of 0.6928 and a root mean square error of 1.2065, outperforming baseline machine learning and deep learning models. The study demonstrated that identifying antenna-related degradation during manufacturing can reduce downstream faults in transmitter and receiver subsystems.

2.2. Existing Fault Detection and Diagnosis Approaches

Once the fault modes and their precursors have been identified, the focus shifts to methods that can reliably detect and diagnose these faults during radar operation. Advances in computational power and algorithm design have enabled the development of sophisticated frameworks capable of fusing multi-source information, extracting complex features from noisy radio frequency (RF) signals, and adapting to evolving fault patterns. The following works illustrate the diversity of detection and diagnosis strategies proposed for radar systems, encompassing adaptive signal decomposition, attention-based deep learning, and comparative evaluations of artificial intelligence techniques.

To address the limitations of traditional Built-In Test Equipment (BITE), which is typically constrained to subsystem-level fault identification and may lead to unnecessary module replacements. Liu et al. proposed a Bayesian network-based fault diagnosis method tailored for radar receiver chains (Liu, Bi, Gu, Wei, & Liu, 2022). Their approach integrates expert knowledge of radar architecture, historical maintenance records, and real-time multi-sensor data, including humidity, temperature, signal phase, current, and voltage, to enable device-level fault localization. The Bayesian network (BN) model represents probabilistic dependencies between fault symptoms and 21 identified fault points, with conditional probability tables derived from empirical data. Applied to operational radar monitoring datasets, the BN-based method demonstrated improved fault localization accuracy, reduced diagnostic costs, and shortened mean time to repair. This highlights the practical benefits of combining probabilistic reasoning with multi-source information fusion.

Building upon earlier studies, Tang et al. introduced a non-invasive diagnostic technique specifically designed for highly integrated multiple-input multiple-output (MIMO) RF front-end modules, where access to internal test points is limited (Tang et al., 2023). Their method consists of three major steps, fault mode identification using Failure Mode and Effects Analysis (FMEA), signal decomposition via Variational

Mode Decomposition (VMD), and classification using an interleaved group convolutional neural network. The VMD enhances fault feature sparsity by reducing model overlap in the frequency domain, while the dual convolutional architecture lowers computational load and parameter count without compromising classification performance. Although this approach captures how hardware degradations alter frequency characteristics, it is primarily used for fault type classification rather than detailed analysis of baseband distortions and radar performance. The method achieved a classification accuracy of 94.44% within 6.4 seconds, demonstrating the effectiveness of combining adaptive signal decomposition with efficient deep learning for rapid fault localization. A complementary technique by Tang et al. employs a deep learning model known as Convolutional Attention Network (CAN) alongside Enhanced Synchro extracting Transform (EST) to generate high resolution time-frequency maps (Tang et al., 2025). This feature-oriented approach processes complex-valued signals and has been validated on a MIMO radar platform. Unlike the earlier method, which prioritizes lower complexity and real-time readiness, this technique emphasizes precision and robustness in feature extraction.

Liu et al. also provided a broader review of machine learning techniques for fault diagnosis in RF and analog circuits (Liu et al., 2022). Their study examined a wide range of algorithms, including artificial neural networks (ANN), support vector machines (SVM), decision trees, and ensemble learning methods such as random forests and boosting techniques. For each method, the authors evaluated key performance dimensions such as diagnostic accuracy, model interpretability, training complexity, and computational efficiency. While not exclusively focused on radar systems, this review offers valuable guidance for selecting appropriate fault diagnosis techniques based on system constraints and application requirements, particularly in RF-intensive environments.

3. SIMULATION METHODOLOGY AND FAULT MODELS

The simulation methodology employed in this study is illustrated in Figure 1, which identifies the three radar subsystems where fault injection is performed: the FMCW waveform generator, the transmitter, and the receiver. Faults are not injected into the digital signal processing (DSP) unit, as it falls outside the scope of this analysis. This section provides a detailed overview of the signal flow and fault injection strategy across the selected subsystems. The simulation focuses on how faults alter the behavior of the radar signal at various stages, enabling a controlled evaluation of fault-induced distortions. Each subsystem is modeled to reflect its functional role in a typical automotive FMCW radar architecture, allowing for targeted fault scenarios that mimic real-world degradation patterns.

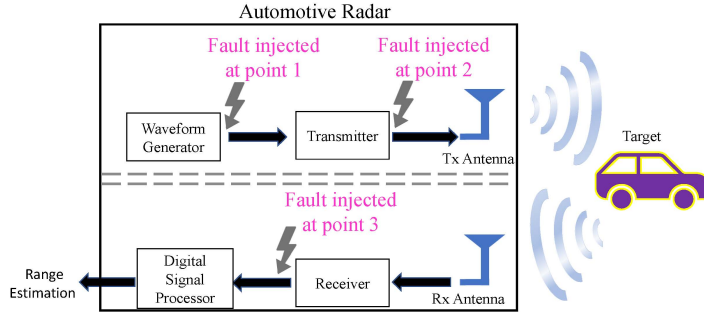


Figure 1. Automotive radar subsystems and fault injection points.

3.1. FMCW Radar Signal Chain

FMCW automotive radar system operates by generating and processing chirp signals, frequency-modulated waveforms that vary linearly over time. These signals are used to estimate the range and velocity of detected targets through beat frequency analysis and Doppler shift measurements. The radar signal chain consists of three primary subsystems where fault signals are injected:

- **Waveform generator:** This unit synthesizes a continuous sequence of linearly frequency-modulated chirps. Each chirp is defined by its start frequency, f_0 , bandwidth B , chirp duration T_c , and slope $S = B/T_c$ in Hz/s, which determines the rate of frequency change. In the ideal case, f_0 increases linearly with time within each chirp period, producing a sawtooth-like frequency-time profile as illustrated in the spectrogram plot in Figure 2b. The waveform signal can be expressed as,

$$s(t) = Ae^{j(2f_0t+St^2)} \quad 0 \leq t \leq T_c, \quad (1)$$

where A is the amplitude of the baseband chirp (see Figure 2a for the Amplitude-time waveform plot).

- **Transmitter:** This converts the generated baseband chirp into an RF signal suitable for propagation through free space. The complex baseband signal is mixed with a local oscillator (LO) to produce an RF signal centered f_c , which is typically 77 GHz in automotive radar applications. The chirp is amplified by a power amplifier (PA) and radiated through the transmit antenna to space. The ideal transmitted waveform maintains the frequency slope and phase linearity of the chirp. Any nonlinearities in the PA or LO leakage introduce spectral distortion. The signal is given as,

$$s_t(t) = A_{RF}e^{j2f_c t} \cdot s(t), \quad (2)$$

where A_{RF} represents the physical RF amplitude gain after all hardware effects up to the antenna port (e.g., filters, amplifiers). The value of A_{RF} can vary with frequency, temperature, and operating point of the PA.

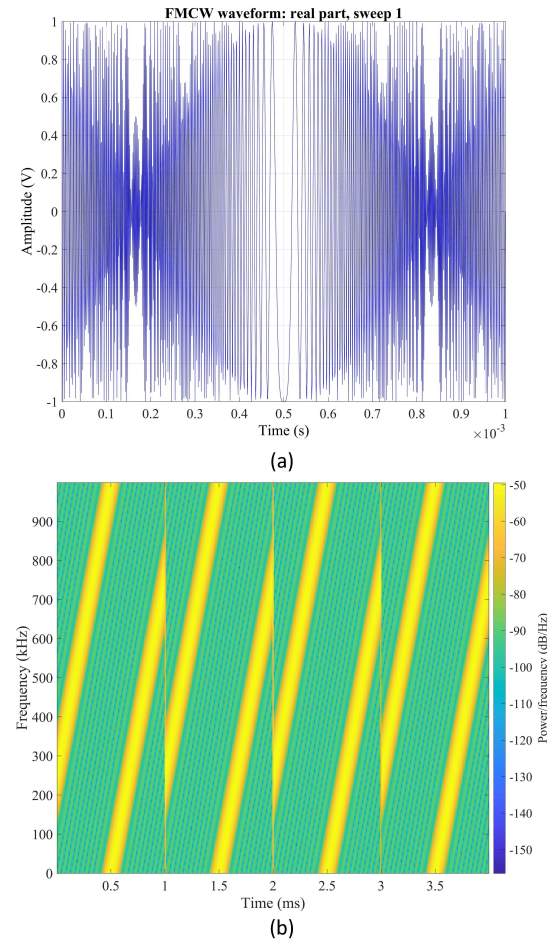


Figure 2. (a) Amplitude–Time and (b) Frequency–Time plot of FMCW waveform.

- **Receiver:** This subsystem captures reflected RF signals from multiple targets and converts them into baseband for digital processing. The incoming RF echo is mixed with a replica of the transmitted chirp, producing an intermediate frequency (IF) beat signal whose frequency is proportional to range of target. A low-pass filter suppresses high-frequency components and noise, isolating the beat frequency f_b . The filtered IF signal is then sampled by an analog-to-digital converter (ADC), resulting in a discrete-time complex baseband signal suitable for range estimation. The transmitted RF chirp, after reflecting off one or more targets, arrives at the receive antenna as,

$$s_r(t) = \sum_{k=1}^K \Lambda_k \cos(2\pi f_c(t - \tau_k) + \pi S(t - \tau_k)^2 + n(t)). \quad (3)$$

After downconverting the received signal, the radar mixes $s_r(t)$ with a copy of the transmitted signal to estimate the baseband received signal as,

$$s_{r_{bb}}(t) = \sum_{k=1}^K \Lambda_k e^{j(2\pi f_b^k t - \pi S \tau_k^2)} + n(t), \quad (4)$$

where K is the number of targets, Λ_k is the attenuation factor for target k , it includes path loss, antenna gain, and radar cross section (RCS) information of the target. τ_k is $2R_k/c$, round trip time delay for range R_k , and c is the speed of light. f_b^k is the beat frequency for target k , directly proportional to R_k . $\pi S\tau_k^2$ is the term for mixing, and lastly, n is additive RF noise.

A clear understanding of the FMCW radar signal chain is essential for analyzing how faults introduced at different stages affect signal integrity and system behavior. Faults in any of these subsystems introduce distortions that propagate through the signal chain, influencing downstream components and overall radar performance. This foundational structure enables targeted fault injection and supports the simulation framework described in the following subsections.

3.2. Simulation Environment

The radar signal chain and fault models were implemented in MATLAB R2024b (The MathWorks Inc., 2024) using the Radar Toolbox (MathWorks, 2024b), Simulink (MathWorks, 2024c), and the Fault Analyzer toolbox (MathWorks, 2024a). The simulation environment involves the automotive radar (waveform generator, transmitter, receiver, and digital signal processor), a target car, and the propagation channel. The general setup of the Simulink simulation is shown in Figure 3.

The radar was configured to operate at 77 GHz, with the chirp parameters, transmitter, and receiver amplifier specifications defined according to the values listed in Table 1. Using parameterized Simulink models in combination with the built-in diagnostic and fault injection capabilities of the Fault Analyzer, faults were systematically introduced into individual radar subsystems while maintaining identical baseline conditions for fair performance comparison. Simulink was chosen for this work due to its ability to integrate high-level algorithm design with detailed physical modeling, enabling accurate signal-level analysis and flexible fault injection within a unified simulation framework.

3.3. Fault Models

The fault injection models considered in this study are sourced from the Fault Analyzer toolbox (MathWorks, 2024a). To simulate realistic degradation scenarios in automotive radar systems, we selected five representative fault behaviors, noise, gain, negate value, offset by one, and unit delay, based on their prevalence in radar hardware failure modes.

Table 1. Simulation Parameters.

Radar	Value
Operating Frequency (GHz)	77
FMCW bandwidth(GHz)	1.5
Sweep duration (s)	0.001
Sample Rate (MHz)	1.5
Tx Reference Impedance (Ohms)	50
Tx PA gain (dB)	30
Tx LNA gain (dB)	40
Signal propagation speed (m/s)	299,792,458
Simulation Duration (s)	0.5
Probability of false alarm	0.0001

These faults reflect common physical and electronic degradation mechanisms, noise reflects thermal and electronic interference in analog components (Moghaddam et al., 2020), gain variations arise from amplifier aging or power instability, negate simulates polarity inversion due to digital logic faults, offset captures DC bias shifts from component drift, and delay represents timing mismatches caused by clock jitter or synchronization loss (Sanches, 2023; Skolnik, 2008). Each fault was individually injected into one of the radar subsystems, waveform generator, transmitter, or receiver, and activated at the start of the simulation. As a result, the fault signals altered the original subsystem signals. Illustrations of these fault behaviors are shown in Figure 4.

The settings and subsystem locations for each fault are summarized in Table 2. Specifically, the noise fault adds a random signal component to the subsystem output, simulating interference or degradation. This results in a distorted version of the original signal, reducing its clarity and potentially masking key features such as frequency or phase. In contrast, a gain fault duplicates the original signal and amplifies its amplitude, resulting in a higher magnitude version of the original signal. A negate fault multiplies the original signal by a negative value, effectively inverting its polarity. This can distort phase relationships and interfere with downstream processing that assumes positive signal orientation. An offset-by-one fault subtracts a constant value of one from the original signal, introducing a fixed bias. This shift can affect amplitude-sensitive operations and degrade signal fidelity. Finally, a de-

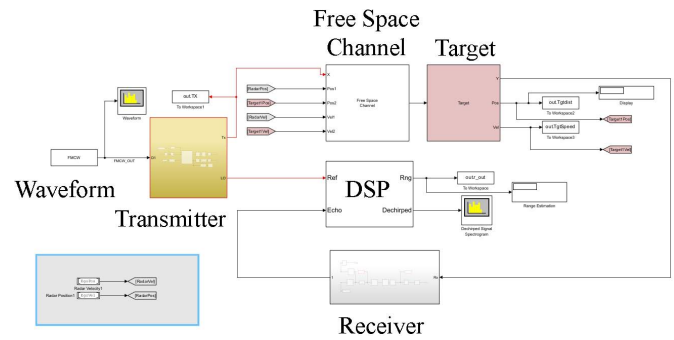


Figure 3. Simulation setup in Simulink.

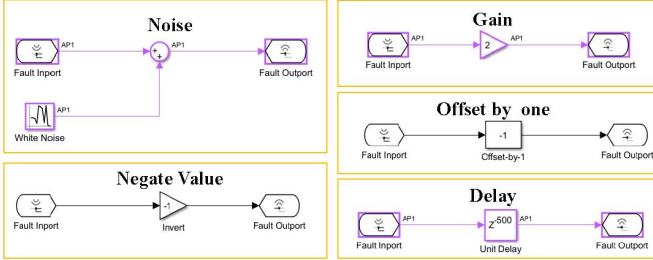


Figure 4. Fault behaviors from Fault Analyzer Toolbox.

Table 2. Fault behavior parameters and settings.

Fault	Behaviors	Parameters	Subsystems	Trigger
1	Noise	Mean = 0, Variance = 1	Waveform, Transmitter (PA), and Receiver (LNA)	Always on
2	Gain	$\times 2$		
3	Negate Value	$\times -1$		
4	Offset by one	$Y = U + \text{Bias}; \text{Bias} = -1$		
5	Delay	500 time steps		

lay fault defers the subsystem output by 500 discrete simulation time steps. This temporal misalignment simulates latency or timing errors, which can disrupt synchronization and impair range or velocity estimation.

3.4. Metrics

The impact of injected faults on radar range estimation is quantified using two primary metrics:

- Mean Squared Error (MSE).

This metric evaluates the deviation between the estimated range and the ground truth. It captures the cumulative effect of signal distortions introduced by faults across the radar processing chain. A higher MSE indicates reduced accuracy in target localization.

- Number of Missing Detections (α).

This metric counts the instances where valid targets fail to be detected due to fault-induced degradation. Missing detections may result from signal attenuation, spectral distortion, or misclassification during digital processing. It serves as a direct indicator of system reliability under fault conditions. Range values with nan output, zero, or negative values are counted as missing detections.

Together, these metrics provide a comprehensive assessment of how faults affect both the precision and robustness of radar-based range estimation.

4. RESULTS AND DISCUSSION

To evaluate the impact of subsystem faults on FMCW radar performance, a controlled simulation scenario was designed with a single target vehicle positioned directly in front of the radar boresight. Five discrete target ranges of 5, 20, 40, 60, and 100 m; and four radial velocities of 0, 5, 10, and 22 m/s were considered, representing typical short to medium-range automotive use cases. For each of the fifteen fault models, comprising five waveform generator faults, five transmitter faults, and five receiver faults, the complete range–velocity set was simulated under identical environmental and radar configuration conditions. This structured experimental design ensured consistent fault isolation as only one fault behavior was injected into the automotive radar sensor at a time.

Starting with the waveform generator, the effects of the faults on the original signal are shown in Figure 5. ¹ In contrast to Figure 2a, the sampling rate was reduced to 5 kHz to better illustrate the actual impact of the fault. Among the fault types, the noise and delay faults caused the most significant disruptions to the original signal. The noise fault introduced spectral distortion and amplitude fluctuations, degrading signal clarity and increasing the likelihood of misinterpretation during processing. The delay fault caused temporal misalignment by shifting the signal in time, resulting in a 500-step lag that disrupted synchronization with the receiver and impaired range estimation accuracy. The remaining faults, gain, negate, and offset, had negligible effects on waveform integrity, with changes that were largely imperceptible in the time-domain signal structure.

Similar fault effects were observed in the transmitter subsystem, as illustrated in Figure 6. While the coupler and power amplifier do not actively attenuate noise, their configuration can influence how injected noise propagates through the signal chain. As a result, some noise components may be partially suppressed, but residual artifacts still persist and contribute to signal degradation.

In contrast, the impact of faults in the receiver subsystem was more pronounced, as shown in Figure 7. The receiver captured additional noise components, including thermal noise and environmental interference, which compounded the distortion introduced by the injected faults. The offset fault significantly reduced the amplitude of the received signal, weakening signal strength and lowering detection reliability. Additionally, delay faults in both the transmitter and receiver introduced a consistent 500 time-step shift in the signal. This temporal misalignment caused the delay plots to appear as displaced replicas of the original waveform, underscoring the disruptive effect of timing faults on radar signal synchronization.

¹Note: For clarity, all waveform plots in Figure 5, 6, and 7 are generated using a 5 kHz downsampled version of the baseband signal. This does not affect the validity of the computed metrics, which are based on the 1.5 MHz sampling frequency.

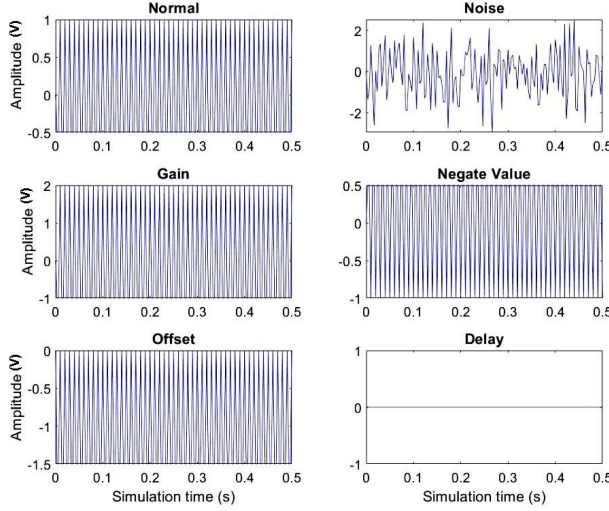


Figure 5. Faults injected in FMCW waveform generator.

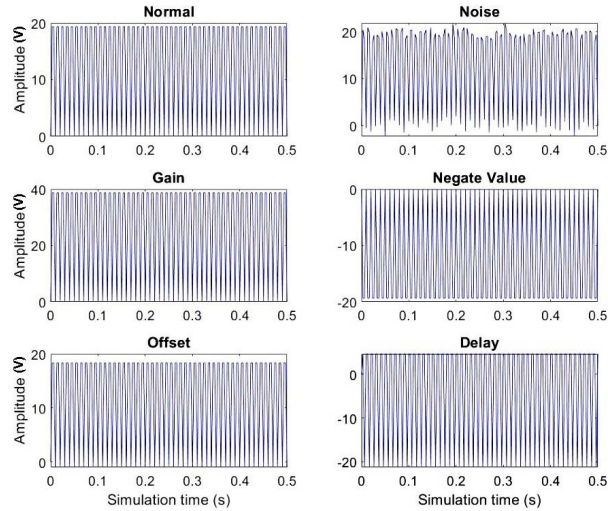


Figure 6. Faults injected in power amplifier of transmitter.

The Fast Fourier Transform (FFT) was applied during range processing with automatic window selection to enhance spectral resolution. Target ranges were estimated using the Cell Averaging Constant False Alarm Rate technique for object detection, with the probability of false alarm set to 1×10^{-4} . The MSE and number of missed detections for fault effects on waveform, transmitter, and receiver are presented in Tables 3, 4, and 5, respectively².

In the waveform generator, delay faults were the most disruptive, producing undefined MSE values and the highest number of missed detections. Offset faults followed with the second-highest average MSE, particularly missing the detection of stationary targets due to amplitude attenuation. Noise

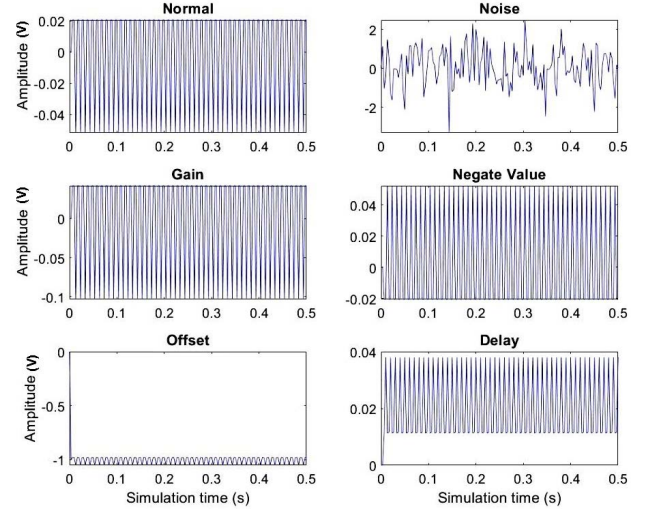


Figure 7. Faults injected in low noise amplifier of receiver.

faults ranked third, contributing to moderate signal distortion and detection failures.

In the transmitter subsystem, noise faults produced the highest average MSE and the most missed detections among the five fault types, indicating significant signal degradation prior to transmission. Delay faults followed, introducing temporal misalignment that moderately affected range estimation and detection accuracy. Offset faults had the least impact in this subsystem, with the lowest average MSE and fewer missed detections.

In the receiver subsystem, offset faults were the most severe, leading to complete signal attenuation, undefined MSE values, and the highest missed detection count (501). Noise faults followed closely, with 470 average missed detections and highest average MSE. Delay faults had a moderate impact. Negate and gain faults across all three subsystems showed no measurable effect. Both resulted in an MSE of 0 and 4 missed detections, indicating no significant alteration to the signal or detection process. It is also important to note that the initial 4 missed detections observed across all subsystems are expected. During the first few consecutive time steps, the radar system requires time to collect and process the initial return signals. As a result, early missed detections are a normal part of the simulation startup behavior and do not reflect fault-induced degradation.

The fault-induced distortions observed in the simulations have significant implications for automotive radar performance in safety-critical scenarios. Noise faults, which consistently produced high MSE and missed detections, pose a serious threat to object recognition and range estimation. Offset fault, particularly in the waveform and receiver subsys-

²It is important to note that in Tables 3 and 5, a dash ("—") is used to represent case where the MSE was either infinite or undefined (NaN). These instances typically occurred under severe fault conditions.

tem, further compromise signal integrity and detection reliability. These vulnerabilities can directly affect core functionalities such as collision avoidance, adaptive cruise control, and lane-keeping assistance. Without fault-aware processing, radar systems may fail silently, thus missing targets or incorrectly estimating ranges without triggering alerts. By identifying distinct fault signatures and quantifying their impact, our findings support the integration of diagnostic intelligence into radar signal chains. Moreover, this fault characterization enhances sensor fusion strategies, allowing systems like LiDAR and cameras to compensate for radar weaknesses. This is especially critical in adverse weather or low-visibility conditions where radar is often the primary sensor. Ultimately, our results contribute to the development of robust, fault-tolerant FMCW radar architectures that can maintain performance and safety even under degraded conditions.

4.1. Generalization to Real Systems

While this study is based entirely on simulated data, the fault behaviors modeled as noise, gain variation, polarity inversion, offset, and delay are grounded in degradation mechanisms commonly observed in real automotive radar systems (Fleck, May, Daniel, & Davies, 2021). These fault types have been documented in industry reports and academic literature as representative of hardware-level anomalies affecting radar signal integrity and performance. Although access to radar measurement hardware is currently limited, the simulation framework provides a controlled and scalable environment for analyzing fault propagation across subsystems. Future work will focus on extending this framework to real radar signal data, contingent on collaboration with radar manufacturers or research institutions equipped with suitable testbeds. Such validation would enable deeper insights into fault manifestation under operational conditions and support the development of fault-tolerant radar processing algorithms.

4.2. Velocity Estimation and Doppler Fault Modeling

Although the primary focus of this study is on range estimation, radar systems also rely on Doppler processing to estimate target velocity. Certain fault behaviors, particularly delay and noise can distort the frequency content of radar returns, leading to inaccurate velocity estimates. In our simulation, we observed that delay faults introduce temporal misalignments, while noise faults inject spectral artifacts that can shift or obscure Doppler peaks. These distortions may result in velocity bias, jitter, or false velocity readings, especially in multi-target scenarios.

While velocity estimation was not evaluated in this study, these preliminary observations highlight the importance of extending fault analysis into the Doppler domain. Future work will incorporate Doppler signal modeling to assess how fault-induced distortions affect velocity estimation accuracy.

Table 3. Range estimation error (MSE) and number of missed detections (α) for each fault injected to the waveform. All MSE values are in m^2 .

Dist (m)	Vel. (m/s)	Noise		Gain		Negate		Offset		Delay	
		MSE	α	MSE	α	MSE	α	MSE	α	MSE	α
5	0	18.39	175	0	4	0	4	24.98	501	-	501
	5	26.65	147	0	4	0	4	36.04	4	-	501
	10	39.56	137	0	4	0	4	54.31	4	-	501
	22	81.86	104	0	4	0	4	117.85	4	-	501
20	0	285.42	165	0	4	0	4	399.62	501	-	501
	5	294.79	97	0	4	0	4	441.74	4	-	501
	10	349.26	106	0	4	0	4	496.16	4	-	501
	22	5269.85	55	0	4	0	4	10241.30	4	-	501
40	0	1061.28	141	0	4	0	4	1598.49	501	-	501
	5	1141.57	84	0	4	0	4	1687.50	4	-	501
	10	1171.21	80	0	4	0	4	1786.86	4	-	501
	22	1333.03	53	0	4	0	4	2071.92	4	-	501
60	0	2207.00	129	0	4	0	4	3596.62	501	-	501
	5	2869.06	66	0	4	0	4	3736.46	4	-	501
	10	2349.88	70	0	4	0	4	3877.77	4	-	501
	22	2500.54	34	0	4	0	4	4290.24	4	-	501
100	0	5366.82	113	0	4	0	4	4990.78	501	-	501
	5	5269.85	55	0	4	0	4	10241.30	4	-	501
	10	6069.96	51	0	4	0	4	10467.03	4	-	501
	22	5425.36	10	0	4	0	4	11131.67	4	-	501

This extension will support the development of fault-tolerant radar algorithms for both range and velocity sensing in automotive applications.

4.3. Multi-Target and Environmental Extensions

The current study simulates a single-target scenario with discrete range and velocity values to isolate and analyze the impact of individual fault types on radar signal integrity. While this controlled setup enables clear attribution of fault effects, real-world automotive environments often involve multiple targets and environmental clutter. These factors introduce additional challenges such as target occlusion, multipath inter-

Table 4. Range estimation error (MSE) and number of missed detections (α) for each fault in the transmitter. All MSE values are in m^2 .

Dist (m)	Vel. (m/s)	Noise		Gain		Negate		Offset		Delay	
		MSE	α	MSE	α	MSE	α	MSE	α	MSE	α
5	0	15142.68	44	0	4	0	4	4.27e-9	4	99.86	4
	5	10047.16	21	0	4	0	4	1.23e-7	4	99.86	4
	10	18074.65	42	0	4	0	4	1.29e-7	4	99.86	4
	22	16526.67	30	0	4	0	4	0.01	4	99.86	4
20	0	14452.04	41	0	4	0	4	6.36e-9	4	99.86	4
	5	14983.74	25	0	4	0	4	3.55e-8	4	99.86	4
	10	17505.40	37	0	4	0	4	1.37e-7	4	99.86	4
	22	15882.81	20	0	4	0	4	6.10e-9	4	99.94	4
40	0	21703.78	43	0	4	0	4	7.01e-9	4	99.86	4
	5	10113.03	16	0	4	0	4	9.34e-9	4	99.86	4
	10	21482.23	48	0	4	0	4	1.47e-7	4	99.85	4
	22	15634.91	31	0	4	0	4	1.48e-7	4	99.85	4
60	0	14494.51	30	0	4	0	4	7.38e-9	4	99.86	4
	5	17172.99	26	0	4	0	4	4.56e-9	4	99.86	4
	10	26453.49	42	0	4	0	4	1.48e-7	4	99.85	4
	22	15185.08	24	0	4	0	4	1.40e-7	4	99.84	4
100	0	21790.91	42	0	4	0	4	7.97e-9	4	99.86	4
	5	15882.81	20	0	4	0	4	6.10e-9	4	99.94	4
	10	21975.71	36	0	4	0	4	1.38e-7	4	99.85	4
	22	19313.26	28	0	4	0	4	3e-3	4	99.99	4

Table 5. Range estimation error ($MSE(m^2)$) and number of missed detections (α) for each fault injected in the receiver. All MSE values are in m^2

Dist. (m)	Vel. (m/s)	Noise		Gain		Negate		Offset		Delay	
		MSE	α	MSE	α	MSE	α	MSE	α	MSE	α
5	0	129086.53	4690	40	4	501	99.86	4			
	5	129011.47	4680	40	4	501	100.70	4			
	10	130346.68	4700	40	4	501	99.87	4			
	22	132250.03	4700	40	4	501	100.06	4			
20	0	135273.24	4700	40	4	501	99.86	4			
	5	135570.63	4700	40	4	501	100.68	4			
	10	135808.33	4700	40	4	501	100.05	4			
	22	166272.21	4700	40	4	501	100.13	4			
40	0	141685.30	4700	40	4	501	99.86	4			
	5	142026.05	4700	40	4	501	100.38	4			
	10	142312.19	4700	40	4	501	99.92	4			
	22	143419.25	4700	40	4	501	100.09	4			
60	0	148896.61	4700	40	4	501	99.86	4			
	5	149290.37	4700	40	4	501	100.30	4			
	10	149658.46	4700	40	4	501	100.15	4			
	22	150828.72	4700	40	4	501	100.04	4			
100	0	165717.09	4700	40	4	501	99.86	4			
	5	166272.21	4700	40	4	501	100.13	4			
	10	166731.84	4700	40	4	501	100.03	4			
	22	168083.95	4700	40	4	501	100.19	4			

ference, and overlapping signal returns, which can amplify or mask the effects of hardware faults.

To extend the applicability of our framework, future work will incorporate multi-target simulations with varying range profiles. This will allow us to evaluate how fault-induced distortions propagate in more complex scenes and affect target discrimination, tracking stability, and false association rates. Additionally, we plan to simulate environmental effects such as ground clutter, rain, and multipath reflections to assess how these external factors interact with internal subsystem faults. These extensions will support a more comprehensive understanding of radar fault resilience under realistic operating conditions.

5. CONCLUSION

This study presents a comprehensive simulation-based investigation into the signal-level impacts of faults within FMCW radar subsystems. By analyzing five representative fault behaviours across the waveform generator, transmitter, and receiver, we demonstrate how each fault uniquely distorts complex baseband signals and affects range estimation performance. Our analysis shows that noise fault is the most detrimental, consistently yielding high MSE and missed detections across all subsystems. Delay and offset faults also significantly impair signal integrity, particularly within the receiver chain. Importantly, we reveal that range errors and missed detections can manifest, challenging conventional assumptions and underscoring the need for fault-aware signal processing. These insights lay the groundwork for future diagnostic frameworks and adaptive algorithms that can detect, isolate, and mitigate fault-induced anomalies in real time. By bridging the gap between fault modeling and signal-level

analysis, this work advances the understanding of radar vulnerability and supports the design of more resilient FMCW radar systems for automotive applications. Looking ahead, we plan to extend our analysis beyond isolated fault scenarios by exploring cross-fault interactions and compound fault behaviors. This will enable a deeper understanding of how multiple simultaneous faults influence radar performance and inform the design of robust, fault-tolerant FMCW radar architectures.

ACKNOWLEDGMENT

This research was supported by Basic Science Research Program through the National Research Foundation of Korea (NRF) funded by the Ministry of Education (NRF-2021R1A6A1A03039493, NRF-2021R1A2 B5B02086773).

REFERENCES

- Bak, S.-H., & Kim, K. P. (2023). An automl-driven antenna performance prediction model in the autonomous driving radar manufacturing process. *KSII Transactions on Internet & Information Systems*, 17(12), 3330–3344. doi: 10.3837/iiis.2023.12.006
- Burza, R. M. (2024). Overview of radar alignment methods and analysis of radar misalignment's impact on active safety and autonomous systems. *Sensors*, 24(15), 4913. doi: 10.3390/s24154913
- Darrah, T., Lövberg, A., Frank, J., & Quinones-Gruiero, M. (2022). Developing deep learning models for system remaining useful life predictions: Application to aircraft engines. In *Proceedings of the phm society conference* (Vol. 14).
- Fleck, S., May, B., Daniel, G., & Davies, C. (2021). Data driven degradation of automotive sensors and effect analysis. *Electronic Imaging*, 33, 1–8.
- Ginsburg, B. P., Subburaj, K., Samala, S., Ramasubramanian, K., Singh, J., Bhatara, S., ... Rentala, V. (2018). A multimode 76-to-81ghz automotive radar transceiver with autonomous monitoring. In *2018 ieee international solid-state circuits conference - (isscc)* (p. 158-160).
- Hou, X., Yang, J., Deng, B., Xia, L., Zhang, Y., & Zhang, Z. (2018). A key lifetime parameters extraction method for t/r module based on association rule. In *2018 international conference on sensing, diagnostics, prognostics, and control (sdpc)* (pp. 165–170). IEEE. doi: 10.1109/SDPC.2018.8664912
- Jankiraman, M. (2018). *Fmcw radar design*. Norwood, MA: Artech House.
- Kraus, F., Scheiner, N., Ritter, W., & Dietmayer, K. (2021). The radar ghost dataset – an evaluation of ghost objects in automotive radar data. In *2021 ieee/rsj international conference on intelligent robots and sys-*

- tems (iros) (p. 8570–8577). IEEE Press. doi: 10.1109/IROS51168.2021.9636338
- Kulevome, D. K. B., Hong, W., Wang, X., Cobbinah, B. M., Agbley, B. L. Y., & Safder, Q. (2021). System diagnosis framework for sustaining the operational fidelity of a radar system. In *2021 18th international computer conference on wavelet active media technology and information processing (ic-cwamtip)* (pp. 640–644). IEEE. doi: 10.1109/IC-CWAMTIP54135.2021.9730812
- Liu, B., Bi, X., Gu, L., Wei, J., & Liu, B. (2022). Application of a bayesian network based on multi-source information fusion in the fault diagnosis of a radar receiver. *Sensors*, 22(17), 6396. doi: 10.3390/s22176396
- MathWorks. (2024a). *Fault analyzer toolbox*. Available online: <https://www.mathworks.com/help/fault-analyzer>. (Accessed: Oct. 2025)
- MathWorks. (2024b). *Radar toolbox*. Available Online: <https://www.mathworks.com/help/radar>. (Accessed: Oct. 2025)
- MathWorks. (2024c). *Simulink*. Available Online: <https://www.mathworks.com/help/simulink>. (Accessed: Oct. 2025)
- Matos, F., Bernardino, J., Durães, J., & Cunha, J. (2024). A survey on sensor failures in autonomous vehicles: Challenges and solutions. *Sensors*, 24(16), 5108. Retrieved from <https://doi.org/10.3390/s24165108> doi: 10.3390/s24165108
- Moghaddam, M. H., Aghdam, S. R., Filippi, A., & Eriksson, T. (2020). Statistical study of hardware impairments effect on mmwave 77 ghz fmcw automotive radar. In *2020 ieee radar conference (radarcon20)* (pp. 1–6).
- Murtala, S., Hur, S., & Park, Y. (2025, February 5). Ghost object detection in automotive radar dataset: An encoder-svm approach. In *Proceedings of symposium of the korean institute of communications and information sciences* (pp. 1,447 - 1,448). South Korea.
- Murtala, S., Lee, I., & Park, Y. (2023). Identification of key parameters for remaining useful life prediction of radar t/r module using least-squares method. In *Phm society european conference* (pp. 86–89). Paris, France: PHM Society.
- Murtala, S., Soojung, H., & Park, Y. (2023). A simplified framework for fault prediction in radar transmitter based on vector autoregression model. In *Phm society asia-pacific conference* (Vol. 4). Tokyo, Japan. doi: <https://doi.org/10.36001/phmap.2023.v4i1.3627>
- Sanches, F. S. (2023). *Analog fault simulation in automotive radar 77 ghz circuit for safety requirements* (Master thesis). University of Jyväskylä, Jyväskylä, Finland.
- Shafique, R., Rustam, F., Murtala, S., Jurcut, A. D., & Choi, G. S. (2024). Advancing autonomous vehicle safety: Machine learning to predict sensor-related accidents severity. *IEEE Access*, 12, 25933-25948. doi: 10.1109/ACCESS.2024.3366990
- Sharif, D., Murtala, S., & Choi, G. S. (2025). A survey of automotive radar misalignment detection techniques. *IEEE Access*, 13, 123314-123324. doi: 10.1109/ACCESS.2025.3584454
- Skolnik, M. I. (2008). Radar handbook. *IEEE Aerospace Electronic Systems Magazine*, 23(5), 41–41.
- Subburaj, K., Ginsburg, B., Gupta, P., Dandu, K., Samala, S., Breen, D., ... Rangachari, S. (2018). Monitoring architecture for a 76-81ghz radar front end. In *2018 ieee radio frequency integrated circuits symposium (rfic)* (p. 264-267). doi: 10.1109/RFIC.2018.8429026
- Tang, X., Liu, Z., Liang, J., Wu, K., Bu, Z., & Chen, L. (2023). A fast fault diagnosis method for rf front-end modules based on adaptive signal decomposition and deep neural network. In *2023 ieee autotestcon* (pp. 1–5). IEEE. doi: 10.1109/AUTOTEST-CON47464.2023.10296419
- Tang, X., Liu, Z., Liang, Y., Lin, Y., Luo, Z., Cheng, Y., & Geng, H. (2025). Ecan: Enhanced-feature extraction and complex asymmetric-convolutional-attention network for intelligent fault diagnosis in mimo system. *IEEE Transactions on Instrumentation and Measurement*. doi: 10.1109/TIM.2025.3554872
- The MathWorks Inc. (2024). *Matlab*. Natick, Massachusetts. Retrieved from <https://www.mathworks.com> (Version 9.13.0 (R2024b))
- Wileman, A. J., & Perinpanayagam, S. (2013). Failure mechanisms of radar and rf systems. *Procedia CIRP*, 11, 56–61. doi: 10.1016/j.procir.2013.07.063
- Zhai, Y., & Fang, S. (2020). A degradation fault prognostic method of radar transmitter combining multivariate long short-term memory network and multivariate gaussian distribution. *IEEE Access*, 8, 199781–199791. doi: 10.1109/ACCESS.2020.3035622
- Zhai, Y., Liu, D., Cheng, Z., & Fang, S. (2022). A novel prognostic model of the degradation malfunction combining a dynamic updated-arima and multivariate isolation forest: Application to radar transmitter. *Electronics*, 11(12), 1921. doi: 10.3390/electronics1112192
- Zhai, Y., Shao, X., Li, J., & Fang, S. (2021). An unsupervised prediction method for radar transmitter degradation fault based on isolation forest. In *Journal of physics: Conference series* (Vol. 2010, p. 012125). IOP Publishing. doi: 10.1088/1742-6596/2010/1/012125
- Zöller, M.-A., Mauthe, F., Zeiler, P., Lindauer, M., & Huber, M. F. (2025). Automated machine learning for remaining useful life predictions. *arXiv preprint arXiv:2306.12215*. Retrieved from <https://arxiv.org/html/2306.12215v2>

BIOGRAPHIES

Sheriff Murtala received his B.Eng. degree in Electrical Engineering from the University of Ilorin, Ilorin, Nigeria, in 2010, and his M.Eng. degree in Communication Engineering from the Federal University of Technology, Minna, Nigeria, in 2017. He earned his Ph.D. in Information and Communication Engineering from Korea University of Technology and Education (KOREATECH), Republic of Korea, in 2021. From 2021 to 2023, he served as a postdoctoral researcher in the Department of Information and Communication Engineering at Yeungnam University, Republic of Korea. Since 2024, he has been with the School of Computer Science and Engineering at Yeungnam University. His research interests include prognostics and health management (PHM) for radar sensors, artificial intelligence and machine learning for autonomous vehicles, and wireless communication systems.

Ingyu Lee received the Ph.D. degree in scientific computing algorithm and software from the Department of Computer Science and Engineering, The Pennsylvania State University. He is currently working as a Research Supervisor with the Sorrell College of Business, Troy University. He is also working as an Assistant Professor with Yeungnam University, South Korea. His research interests include developing efficient scientific computing algorithms based on mathematical modeling using high performance computing architectures and their applications to real world problems includ-

ing information retrieval, data mining, and social networking. He is also a member of IEEE Society.

Soojung Hur received the B.S. degree from Daegu University, Gyeongbuk, South Korea, in 2001, the M.S. degree in electrical engineering from San Diego State University, San Diego, in 2004, and the M.S. and Ph.D. degrees in information and communication engineering from Yeungnam University, South Korea, in 2007 and 2012, respectively. She is working as a Research Professor with the Mobile Communication Laboratory, Yeungnam University. Her current research interests include the performance of mobile communication, indoor/outdoor location, and unnamed vehicle.

Gyu Sang Choi received the Ph.D. degree in computer science and engineering from The Pennsylvania State University. He was a Research Staff Member at the Samsung Advanced Institute of Technology (SAIT), Samsung Electronics, from 2006 to 2009. Since 2009, he has been working with Yeungnam University, where he is currently working as an Assistant Professor. His research interests include data mining, deep learning, computer vision, storage systems, parallel and distributed computing, supercomputing, cluster-based web servers, and data centers. He is now mainly working on text mining and reinforcement learning, deep learning with computer vision, while his prior research has been mainly focused on improving the performance of clusters. He is a member of ACM. He is also a member of IEEE Society.